Exact field ionization rates in the barrier-suppression regime from numerical time-dependent Schrödinger-equation calculations

D. Bauer and P. Mulser
Theoretical Quantum Electronics (TQE), Darmstadt University of Technology, Hochschulstrasse 4A, D-64289 Darmstadt, Germany*
(Received 24 February 1998; revised manuscript received 6 April 1998)

Numerically determined ionization rates for the field ionization of atomic hydrogen in strong and short laser pulses are presented. The laser pulse intensity reaches the so-called ''barrier-suppression ionization'' regime where field ionization occurs within a few half laser cycles. Comparison of our numerical results with analytical theories frequently used shows poor agreement. An empirical formula for the ''barrier-suppression ionization'' rate is presented. This rate reproduces very well the course of the numerically determined ground-state populations for laser pulses with different length, shape, amplitude, and frequency.
[S1050-2947(99)04001-9]

PACS number(s): 32.80.Rm

I. INTRODUCTION

With the ''table-top'' laser systems, nowadays available, laser pulse peak field strengths much greater than the binding field of the outer atomic electrons can be achieved (see, e.g., [1] for an overview). Above a certain threshold electric field the electron is able to escape even classically from the atomic nucleus, i.e., without tunneling through the barrier formed by the Coulomb potential and the external electric (laser) field. This regime is called ''barrier-suppression ionization'' (BSI) [2].

In combination with the dramatic progress in decreasing the pulse duration below 10 fs [3–6] new features in the ionization dynamics are expected. In particular, ionization at such high field strengths occurs mainly within a few half laser cycles, i.e., on a subfemtosecond time scale, provided that the pulse rises fast enough so that tunneling contributes negligibly to the overall ionization. Fast depletion of bound states within one half laser cycle leads to a nonisotropic electron distribution. Apart from the peaked angular distribution of the photo electrons in electric field direction, in the BSI case there is also an asymmetry along this field axis [7]. This opens up the possibility to manipulate the electron distribution function of laser produced plasmas. By ''tailoring'' the pulse shape the plasma formation process may be controlled according to the application under consideration, e.g., harmonics generation [8], or x-ray laser schemes [9].

Experimentally observed ion yields are usually analyzed by means of tunneling theories among these Ammosov-Delone-Krainov (ADK) [10], Keldysh [11], Keldysh-Faisal-Reiss (KFR) [12], or Landau [13] theory are the most prominent ones. However, it is, in general, not possible to get good agreement for several ion species without ''shifting'' the laser intensity [2]. By examining the derivations of KFR-type theories it becomes obvious that they *should* fail in the barrier-suppression ionization regime because the transition between an *unperturbed* initial state and a Volkov state is calculated there. However, the influence of the strong laser field on the *inner atomic* dynamics must not be neglected in BSI. An attempt to extend the ADK theory to BSI has been undertaken [14]. A pure classical ionization rate has been proposed recently [15].

In this paper we compare numerically determined ionization rates for various kinds of pulse shapes and peak field strengths with results predicted by several analytical derivations: the Landau tunneling formula [13], the Keldysh rate [11], the ADK formula [10] and its extension to the BSI regime [14], a classical rate derived by Posthumus *et al.* [15] and a tunneling rate suggested by Mulser [16]. In our numerical studies we restrict ourselves to the ionization of atomic hydrogen in an intense, short, linearly polarized laser pulse. We focus on the field strength region where the ionization rate is of the order of the laser frequency because ionization occurs within a few half laser cycles in this case.

In Sec. II we review the time-dependent Schrödinger equation (TDSE) of field ionization. Moreover, we state the analytical formulas used for comparison with our numerical results. In Sec. III we present our numerical results for various pulse shapes and field strengths. The numerical results are discussed in Sec. IV. We conclude in Sec. V. Details on the numerical method are attached in the Appendix.

II. THEORY

A. Time-dependent Schrödinger equation

The TDSE for an electron interacting with the nuclear potential $-Z/r$ and the laser field $\boldsymbol{E}(t)$ in dipole approximation and length gauge reads (see, e.g., [17])

$$i\frac{\partial}{\partial t}\Psi(\boldsymbol{r},t)=\left(-\frac{\nabla^2}{2}-\frac{Z}{r}+\boldsymbol{r}\boldsymbol{E}(t)\right)\Psi(\boldsymbol{r},t) \tag{1}$$

[atomic units (a.u.) are used throughout this paper [18]]. If the electric field is chosen to be directed along the z axis, cylindrical coordinates are introduced, and the ansatz $\Psi(\rho,\varphi,z,t)=\psi(\rho,z,t)\exp(im\varphi)(2\pi)^{-1/2}$ is made, the TDSE assumes the following two-dimensional form:

*URL: http://www.physik.tu-darmstadt.de/tqe/

$$i\frac{\partial}{\partial t}\psi=-\frac{1}{2}\left[\frac{1}{\rho}\frac{\partial}{\partial\rho}\left(\rho\frac{\partial}{\partial\rho}\right)-\frac{m^2}{\rho^2}+\frac{\partial^2}{\partial z^2}\right]\psi+\left(zE(t)-\frac{Z}{\sqrt{\rho^2+z^2}}\right)\psi, \tag{2}$$

and the normalization condition

$$\int_0^\infty d\rho\,\rho\int_{-\infty}^{\infty}dz\,|\psi(\rho,z,t)|^2=1 \tag{3}$$

holds. The TDSE (2) was numerically solved first by Kulander in 1987, but for intensities below 10^{15} W/cm^2 [19].

In a recent work by Kono *et al.* [20] it was systematically examined for what parameter λ the substitution

$$\Phi(\xi,z,t)=\sqrt{\lambda}\,\xi^{\lambda-1/2}\psi(\xi^\lambda,z,t),\quad \xi^\lambda=\rho, \tag{4}$$

is most favorable numerically. It turned out that the choice $\lambda=3/2$ is best, both for stability and accuracy. The TDSE corresponding to the substitution (4) is given in the Appendix. We used a Peaceman-Rachford scheme to propagate the wave function $\Phi(\xi,z,t)$ (see the Appendix or Ref. [20] for details). Absorbing boundary conditions were implemented which keep the main interaction region in the vicinity of the atomic nucleus free from otherwise reflected probability density.

In all our calculations we started from the $1s$ ground state, i.e., $m=0$. The stable ground state on the numerical grid (which is slightly different from the analytical solution of the Coulomb problem, depending on the grid spacing) was determined by applying our propagation scheme with an imaginary time step to the grid representation of the known analytic solution.

B. Ionization rate formulas

In this section we review the ionization rate formulas used for comparison with our numerical results of Sec. III. If we assume that an ionization rate $W[E(t)]$ is given, the probability for the electron to remain bound is

$$\Gamma(t)=\exp\left(-\int_0^t W[E(t')]dt'\right). \tag{5}$$

We take

$$\Lambda(t)=1-\Gamma(t) \tag{6}$$

as the ionization probability which is, apart from a small time shift, equivalent to the common procedure to calculate the amount of probability to find the electron in a small volume around the atomic nucleus,

$$\Lambda'(t)=1-\int_0^a d\rho\,\rho\int_{-a}^{a}dz\,|\psi(\rho,z,t)|^2,\quad a\approx 5\ \text{a.u.} \tag{7}$$

We assume that the laser pulse ''hits'' the atom at $t=0$ (or ionization is negligible for $t<0$).

1. Landau formula

Landau and Lifshitz derived a formula for the ionization rate of hydrogen when the electron is in the ground state initially [13]. The result is easily extended to hydrogenlike ions (where the ground-state energy is $\mathcal{E}_0=-Z^2/2$),

$$W_{\rm L}=4\frac{(2|\mathcal{E}_0|)^{5/2}}{E}\exp\left(-\frac{2(2|\mathcal{E}_0|)^{3/2}}{3E}\right). \tag{8}$$

2. Keldysh formula

Keldysh perturbatively calculated the transition rate from an initial bound state to a state representing a free electron in a laser field (Volkov state) [11],

$$W_{\rm K}=\frac{(6\pi)^{1/2}}{2^{5/4}}\mathcal{E}_0\left(\frac{E}{(2\mathcal{E}_0)^{3/2}}\right)^{1/2}\exp\left(-\frac{2(2|\mathcal{E}_0|)^{3/2}}{3E}\right). \tag{9}$$

3. Ammosov-Delone-Krainov formula

Ammosov, Delone, and Krainov derived a tunneling ionization rate for complex atoms in an ac electric field [10]. The initial state is described by an effective quantum number n^* and the angular and magnetic quantum numbers ℓ and m, respectively. The ADK result reads

$$W_{\rm ADK}=C_{n^*\ell}^2 f(\ell,m)|\mathcal{E}_0|\left(\frac{3E}{\pi(2|\mathcal{E}_0|)^{3/2}}\right)^{1/2}\times\left(\frac{2}{E}(2|\mathcal{E}_0|)^{3/2}\right)^{2n^*-|m|-1}\exp\left(-\frac{2(2|\mathcal{E}_0|)^{3/2}}{3E}\right), \tag{10}$$

with

$$C_{n^*\ell}=\left(\frac{2e}{n^*}\right)^{n^*}(2\pi n^*)^{-1/2},$$

$$f(\ell,m)=\frac{(2\ell+1)(\ell+|m|)!}{2^{|m|}|m|!(\ell-|m|)!}.$$

The constant e in the coefficient $C_{n^*\ell}$ is Euler's number 2.718 28 . . . . In the derivation of the ADK rate (10) averaging over one laser cycle was performed. The validity of the ADK formula is expected to be best for $n^*\gg 1$, $E\ll 1$, and $\omega\ll|\mathcal{E}_0|$.

4. BSI extension to ADK

Krainov suggested an extension of ADK theory to incorporate BSI [14]. The result is

$$W_{\rm Kr}=\frac{4\sqrt{3}}{\pi n^*}\frac{E}{(2E)^{1/3}}\left(\frac{4e(|\mathcal{E}_0|)^{3/2}}{En^*}\right)^{2n^*}\times\int_0^\infty \mathrm{Ai}^2\left(x^2+\frac{2|\mathcal{E}_0|}{(2E)^{3/2}}\right)x^2dx, \tag{11}$$

where Ai denotes the Airy function. Formula (11) reduces to the usual ADK rate (10) in the limit of a relatively weak laser field (tunneling limit).

5. Classical rate proposed by Posthumus et al.

Recently, Posthumus and co-workers proposed a purely classical BSI ionization rate [15]. Taking the equipotential surface corresponding to the atomic ground state and examining its intersection with the field-deformed Coulomb potential enables the authors to calculate the rate from a geometrical viewpoint. Their result reads

$$W_{\rm cl}=\frac{1-\mathcal{E}_0^2/(4ZE)}{2T_0},\quad T_0=\frac{\pi Z}{|\mathcal{E}_0|(2|\mathcal{E}_0|)^{1/2}}. \tag{12}$$

T_0 is the classical orbit period for the so-called ''free-falling'' trajectories with zero angular momentum. The authors of [15] present also a cycle-averaged expression of the rate. They finally suggest to take $W_{\rm cl}+W_{\rm ADK}(I_{\rm cl})$ as the total ionization rate in the BSI regime where $I_{\rm cl}$ is an appropriate threshold intensity.

6. Tunneling rate proposed by Mulser

Mulser calculated the ionization rate by approximating the tunneling barrier formed by the Coulomb potential and the external field with a barrier parabolic in shape [16]. After calculating the transmission coefficient through this parabolic barrier and making an assumption for the tunneling current the rate formula

$$W_{\rm Mu}=\frac{|\mathcal{E}_0|}{|\beta|}\ln\frac{A+\exp|\beta|}{A+1},\quad \text{where } A=\exp\left(-\frac{7-3\alpha}{4}C\right), \tag{13}$$

$$\beta=\frac{3+\alpha}{4}C,\quad \alpha=\frac{4E^{1/2}}{(2|\mathcal{E}_0|)^{3/4}},\quad C=-\pi(2|\mathcal{E}_0|)^{1/8}\frac{2|\mathcal{E}_0|}{2^{1/2}E^{3/4}}$$

is obtained.

III. NUMERICAL RESULTS

In this section we study the ionization dynamics of the $1s$ atomic hydrogen electron under the influence of the external laser field $E(t)$. The laser field is assumed to have the form

$$E(t)=\hat{E}(t)\sin(\omega t+\varphi), \tag{14}$$

where $\hat{E}(t)$ is the pulse shape function and φ is a constant phase. In the following we vary the pulse envelope $\hat{E}(t)$, the laser frequency ω, and the phase φ in order to examine their influence on the temporal evolution of the ground-state probability $\Gamma(t)$.

A. Instantaneously switched on dc field

Although the dc field instantaneously switched on is, from the experimental point of view, not realistic at all, this case delivers useful insight into how important transient effects might be. Furthermore, it is interesting to check whether ionization occurs with a constant rate after transient effects have died out.

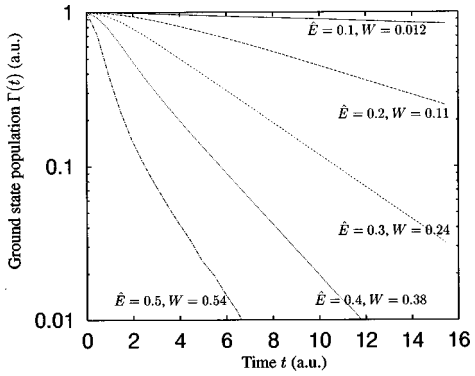

FIG. 1. Ground-state population $\Gamma(t)$ vs time for an instantaneously switched on dc electric field. After a short transient behavior (until ≈ 2 atomic time units) the rates remain constant in time. The field strengths $\hat{E}$ as well as the constant rates W are indicated in the plot.

In the instantaneously switched on field case the envelope function is

$$\hat{E}(t)=\hat{E}=\text{const}\quad \text{for } t>0\quad (0 \text{ otherwise}). \tag{15}$$

In Fig. 1 the ground-state population $\Gamma(t)$ is plotted vs time for the five different amplitudes $\hat{E}=0.1$, 0.2, 0.3, 0.4, and 0.5. One easily verifies that after a very short transient period of about 2 a.u.$=0.048$ fs the constant rate behavior sets in. This transient time period may be estimated by purely classical considerations if one assumes that the atomic response time is similar to that of a classical system with an electron density corresponding to the quantum mechanical probability density of the ground state. The electron density then is $n_e \approx (4\pi/3)^{-1}$ a.u., which leads to a ''plasma frequency'' $\omega_p \approx 3^{1/2}$ a.u. The classical response time therefore would be about 3.6 a.u.$=0.09$ fs.

The constant rates W are given in the plot. We postpone a comparison with the analytical rate formulas mentioned above till Sec. IV.

The probability density $|\psi(\xi,z)|^2$ after 15.5 atomic time units for the $\hat{E}=0.3$ case is shown in Fig. 2. Since we chose $\hat{E}>0$ the electron escapes in negative z direction. Note the pronounced asymmetry and the $1s$ peak which does not move as a whole; it rather persists at the Coulomb singularity.

B. Square pulses and phase dependence

Now we study an ac field with a steplike envelope function,

$$E(t)=\hat{E}\ \sin(\omega t+\varphi)\quad \text{for}\quad t>0\quad (0\ \text{otherwise}). \tag{16}$$

In Fig. 3 the ground-state populations for the two field amplitudes $\hat{E}=0.3$ and 0.5 are shown. In each case three different phases ($\varphi=0,\pi/4,\pi/2$) were chosen in order to check

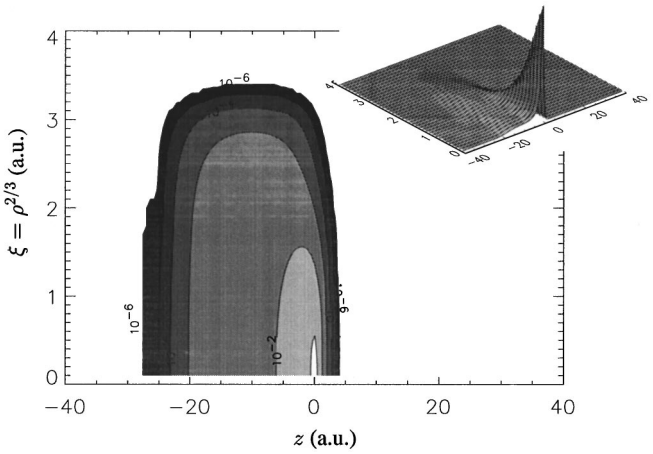

FIG. 2. Contour plot of the probability density $|\psi(\xi,z)|^2$ after 15.5 atomic time units for the $\hat{E}=0.3$ case. The inlet shows the same situation as a surface plot. The electron escapes in negative z direction by ''over the barrier'' ionization. However, a peak remains at the Coulomb singularity.

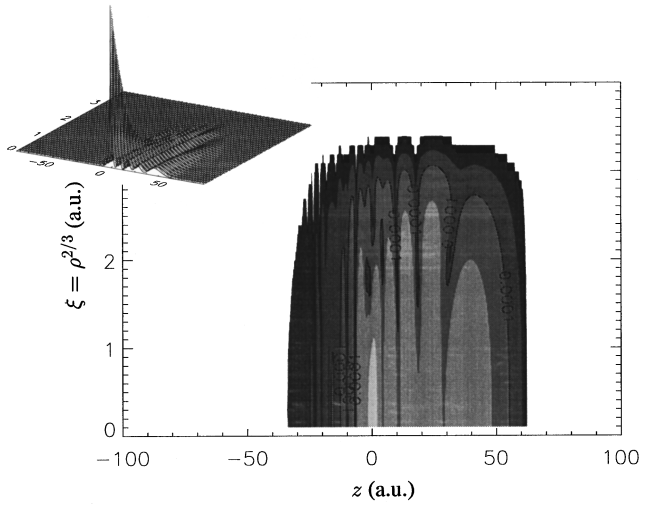

FIG. 4. Contour plot of the probability density $|\psi(\xi,z)|^2$ after one laser cycle for the $E(t)=0.3\cos\omega t$ case. Owing to rescattered probability density wave packets have already formed. The inlet shows the corresponding surface plot of the probability density.

how strong ionization depends on phase effects. The frequency was $\omega=0.2$ in these runs.

During the course of one half cycle ionization is strongly phase dependent. In the $E(t)=\hat{E}\cos\omega t$ cases ionization is particularly strong in the beginning owing to the abrupt turn on of the field, while in the $E(t)=\hat{E}\sin\omega t$ cases ionization starts smoothly. A steady state rate, based on cycle averaging, of course cannot resolve such details.

For $\hat{E}=0.3$ ionization lasts mainly two half cycles while for $\hat{E}=0.5$ already after one single half cycle ionization is $>98\%$. The more rapid ionization is, the stronger should be the dependence of ionization on the phase φ. However, even in the $\hat{E}=0.5$ case the two fields $E(t)=\hat{E}\sin\omega t$ and $E(t)=\hat{E}\cos\omega t$ lead to the same net ionization *after one half cycle*. Only if one is interested in the ionization dynamics on time scales below one optical half cycle ionization becomes phase sensitive. However, even the shortest pulses nowadays

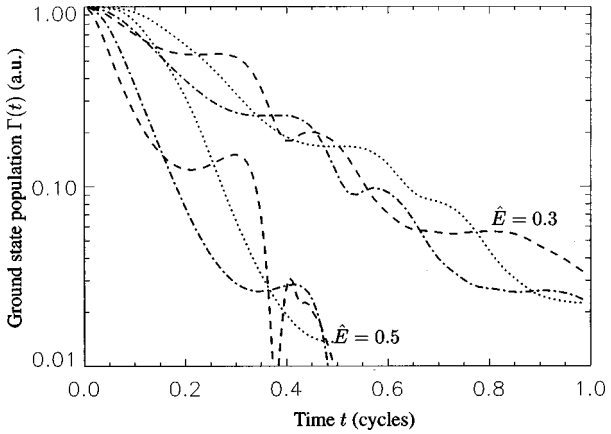

FIG. 3. The ground-state populations in a strong ac field for two different peak field strengths ($\hat{E}=0.3$ and 0.5) and three different phases φ each. The dotted lines correspond to $\varphi=0$, i.e., $\hat{E}\sin\omega t$, the dashed lines are the $\varphi=\pi/2$ case ($\hat{E}\cos\omega t$), and the intermediate case $\varphi=\pi/4$ is drawn dashed-dotted.

available have to cross the field strength region where the ionization rate is $\approx\omega$. Once this regime is passed there is not much electron density left to be ionized by the stronger part of the pulse.

For the sake of illustration the probability density after one complete optical cycle in the $E(t)=0.3\cos\omega t$ case is shown in Fig. 4. Owing to rescattering of probability density at the ionic core wave packets have already built up. Closer examination yields that subsequent wave packets in position space can be mapped to subsequent wave packets in momentum space. These momentum space packets differ in energy by the amount of $\hbar\omega$, and thus are the famous ''above threshold ionization'' (ATI) peaks (see [21] for a detailed analysis).

C. Gaussian pulses

A shape which resembles in a reasonable manner an experimental laser pulse is Gaussian. We took

$$E(t)=\hat{E}(t)\sin\omega t,\quad \hat{E}(t)=\hat{E}\exp\left(-\frac{(t-t_0)^2}{4\sigma^2}\right). \quad (17)$$

Since a Gaussian is infinitely extended we have to start our computer runs with nonvanishing $\hat{E}(0)$. We chose $\hat{E}(0)$ to be 5% of the maximum field amplitude $\hat{E}$. Demanding the Gaussian envelope to cover N laser cycles within the region $\hat{E}(t)>0.05\hat{E}$ yields

$$t_0=N\pi/\omega,\quad \sigma^2=t_0^2/(4\ln 20). \quad (18)$$

In Fig. 5 the ground-state populations for the four Gaussian pulses with $\hat{E}=0.3$, 0.5 and $N=6$, 12 each and $\omega=0.2$ are shown. Besides, the result for a lower frequency ($\omega=0.1$) and $\hat{E}=0.5$, $N=12$ is included. The 12-cycle $\hat{E}=0.3$ pulse (drawn solid) ionizes most slowly, but the six-cycle $\hat{E}=0.3$ pulse (dotted) depletes the ground state quicker than is the

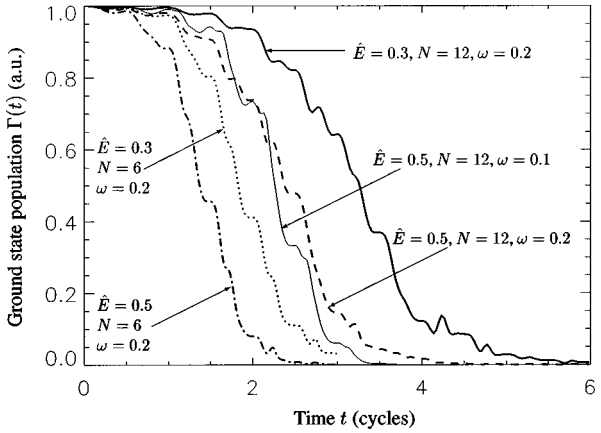

FIG. 5. Ground-state populations for hydrogen in a Gaussian laser pulse covering N cycles within the region where the electric field is 5% of the pulse amplitude $\hat{E}$ [see formulas (17) and (18) for details].

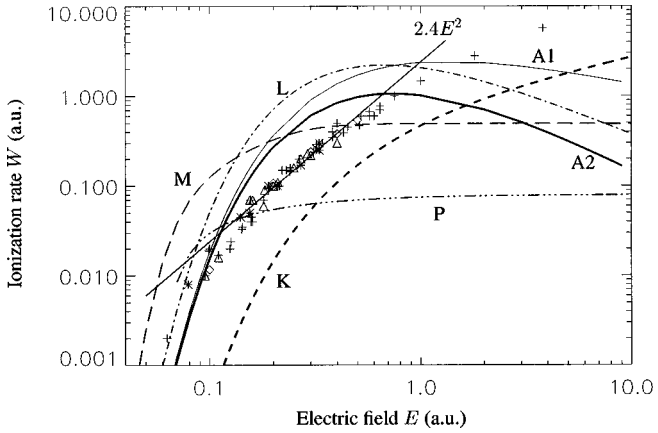

FIG. 6. Instantaneous ionization rates vs the electric field present at the certain instant during the course of the laser pulse. The results have been obtained from different pulse shapes and frequencies: (+) $\sin^2$ pulse with $\omega=0.2$, (*) $\sin^2$ pulse with $\omega=0.1$, ($\diamond$) instantaneously switched on dc field, ($\triangle$) Gaussian pulse with $\omega=0.2$. The curves are predictions from various analytical theories: (L) Landau, (A1) ADK, (A2) to BSI extended ADK, (K) Keldysh, (P) Posthumus, and (M) Mulser. The agreement in the region $0.15 \leqslant E \leqslant 0.5$ is poor. The straight line is $W=2.4E^2$ which fits the numerical data in this region quite well.

case for the 12-cycle $\hat{E}=0.5$ case (dashed). This is due to the fact that the BSI regime is reached earlier for the weaker but shorter $\hat{E}=0.3$ pulse.

The low frequency pulse (thin solid line) causes more rapid ionization than its counterpart with twice the frequency since the total time where the BSI region is reached (measured in *absolute* time units) is larger.

We will further discuss the ground-state populations depicted in Fig. 5 in Sec. IV when we reproduce them with an empirical formula.

D. $\sin^2$ pulses

In Ref. [7] one of the authors dealt extensively with $\sin^2$ pulses of the form

$$E(t)=\hat{E}\,\sin^2\left(\frac{\pi}{T}t\right)\sin\,\omega t, \quad T=N\frac{2\pi}{\omega}. \tag{19}$$

Since the results look very similar to those in the Gaussian case we suppress a further discussion here. However, in Sec. IV we utilize rates numerically determined in [7] for $\sin^2$ pulses in order to confirm the insensitivity of our proposed rate formula with respect to the pulse shape. Furthermore, a different numerical scheme was used in [7]. This gives additional reliability to the numerical results which will be utilized to derive an empirical BSI rate in the following section.

IV. DISCUSSION

In this section we want to demonstrate that it is possible to reproduce our numerical results using a simple formula for the ionization rate in the BSI regime. This rate is not sensitive to laser frequency and pulse shape in a wide parameter range. Moreover we show that none of the analytical rates stated in Sec. II B is applicable to BSI.

Since BSI occurs mainly during one or two half laser periods a cycle-averaged rate obviously makes no sense. Therefore the laser field $E(t)$ with its entire time dependence has to be plugged into a rate formula, i.e., $W(t)=W[E(t)]$, while in tunneling ionization a rate which depends on the pulse envelope only, $W(t)=W[\hat{E}(t)]$, is sufficient.

We determined *instantaneous* ionization rates from the decreasing ground-state populations, in accordance with Eq. (6). In Fig. 6 the results are plotted vs the electric field present at the corresponding instant. Usually the deepest descent in the ground-state population is in the vicinity of the electric field maximum of the actual half cycle. However, this behavior might be disturbed by ''backsweeping'' probability density ionized earlier, especially for high frequencies (frequencies not much less than $|\mathcal{E}_0|$) since the excursion length of a freely oscillating electron is then not much larger than the width of its wave packet representation.

In Fig. 6 different symbols are used for different pulse shapes, pulse lengths, and laser frequencies. For comparison the predictions by the analytic formulas of Sec. II B are drawn as well. The scattering of the numerical data is due to the fact that instantaneous rates for a certain electric field value may stem from runs with different pulse shapes, peak field strengths, or laser frequencies.

The BSI regime for atomic hydrogen sets in for $E=0.146$ when a classical electron, initially on an $\mathcal{E}_0=-0.5$ orbit, can escape from the atomic core. In general this so-called *critical field* in the case of hydrogenlike ions is given by [22–24]

$$E_{\rm crit}=(\sqrt{2}+1)|\mathcal{E}_0|^{3/2}. \tag{20}$$

Once the critical field is reached one expects rapid ionization within a few half cycles. Therefore we are especially interested in the region where $E \geqslant 0.15$. Fortunately, the scattering of our numerical data is small in this region of field strengths. This makes possible our goal to provide a BSI rate formula valid for a wide range of pulse shapes and laser frequencies.

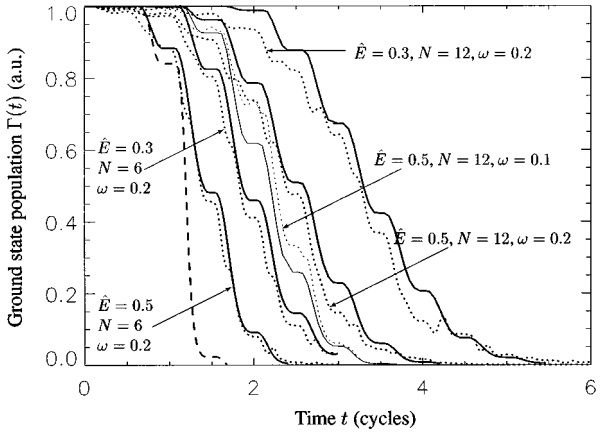

FIG. 7. Comparison of the numerically determined ground-state populations vs time (drawn dotted) with the analytical predictions by means of the empirical formula (21) (drawn solid). The dashed curve shows the result for the $\hat{E}=0.5$, $N=6$ result when only the Landau rate (8) is applied during the entire pulse.

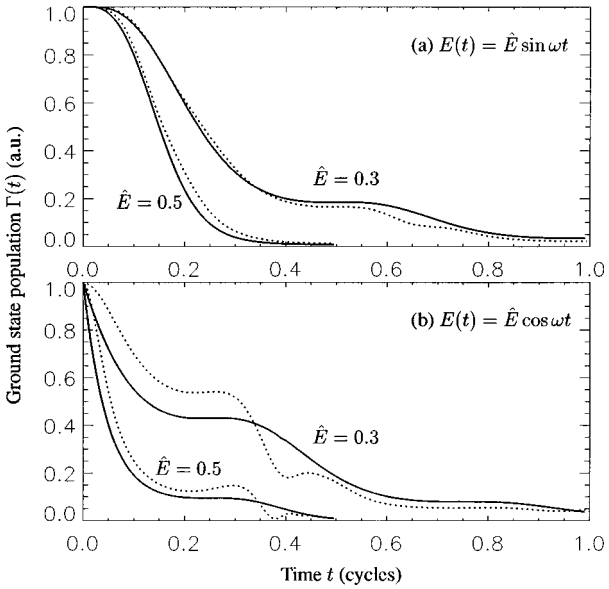

FIG. 8. Comparison of the numerical square pulse results with the predictions by formula (21). In the upper plot (a) the agreement is very good while in the lower plot (b) formula (21) suffers from the transient ionization dynamics caused by the abrupt jump in the electric field at $t=0$.

We observe that none of the analytical theories under consideration predicts the BSI rates correctly. Apart from Keldysh's result all formulas overestimate the ionization rate in the region of interest, $0.15 \leqslant E \leqslant 0.5$. The ionization rate for much higher field strengths might be of academic interest since such high field strengths cannot be reached without strongly ionizing the hydrogen atom during earlier parts of the pulse where the field strength is in the region we focus on in this paper. In real experiments, with rare gases for instance, there are of course stronger bound electrons which get free not before $E \gg 0.1$ but for those electrons E_{crit} is larger too. We will discuss the scaling behavior of the ionization rate with respect to Z later on.

The rates of Posthumus (P) and Mulser (M) saturate at higher field strengths. This is owing to taking the *unperturbed* inner atomic motion to derive an ionization current. In reality, however, the external field influences the inner atomic motion of the electron and yields a higher ionization current. The tunneling theories (L, A1, and A2) are even worse when extrapolated to higher field strengths; they predict a decreasing ionization rate which is clearly unphysical. Note that ''stabilization'' cannot occur when ionization lasts less than one laser cycle. Although the Keldysh rate (K) does not suffer from these shortcomings it underestimates the ionization rate by a factor 3 and more.

The numerically determined ionization rates in the region $0.15 \leqslant E \leqslant 0.5$ can be nicely fitted by $W=2.4E^2$. Since every realistic pulse passes through a region where the electric field is within the tunneling regime we propose a combined formula

$$W(t)=\begin{cases} W'[E(t)] & \text{for } E(t)<E' \\ 2.4E(t)^2 & \text{for } E(t)\geqslant E', \end{cases} \tag{21}$$

where E' is a threshold electric field determined by imposing $W(t)$ to be continuous, and $W'(t)$ is an appropriate tunneling rate. For the Landau rate $E'=0.084$ holds.

In Fig. 7 the solid curves were calculated by applying the BSI rate (21) to the four Gaussian pulses which led to the results already depicted in Fig. 5. For W' we used the Landau tunneling rate. The agreement with the exact numerical results (drawn dotted) is satisfactory. Deviations, especially in the $N=12$, $\hat{E}=0.3$ run, are mainly due to the (even for lower field strength) not very accurate Landau rate. For shorter pulses and higher peak field strengths the agreement becomes excellent. The dashed curve is the result when the Landau rate alone is applied to the entire $N=6$, $\hat{E}=0.5$ pulse; the ionization rate is strongly overestimated.

In Fig. 8 the BSI rate (21) was evaluated for the square pulses discussed in Sec. III B. In the upper plot the agreement with the numerical results for the $\hat{E}$ sin ωt case is good. However, in the lower plot ($\hat{E}$ cos ωt case) the agreement is not particularly good since the abrupt jump in the field strength from 0 (for $t \leqslant 0$) to $\hat{E}$ for $(t>0)$ leads to transient dynamics which cannot be reproduced by our simple rate (21). Therefore care has to be excercised for laser pulses where the BSI regime is reached rather abruptly on time scales shorter than one quarter laser cycle. In all other cases the rate formula (21) worked well.

A. Scaling

The TDSE (1) can be rescaled to the atomic hydrogen case by substituting

$$\tilde{\boldsymbol{r}}=Z\boldsymbol{r}, \quad \tilde{t}=Z^2 t, \quad \tilde{\omega}=\omega/Z^2, \quad \tilde{\boldsymbol{E}}=\boldsymbol{E}/Z^3. \tag{22}$$

Since our BSI rate is not sensitive to ω, and an ionization rate has the dimension of an inverse time the rescaled result reads

$$W(t)=\begin{cases} W'[E(t)] & \text{for } E(t)<E' \\ (2.4/Z^4)E(t)^2 & \text{for } E(t)\geqslant E'. \end{cases} \tag{23}$$

B. The role of the Keldysh parameter

The Keldysh parameter

$$\gamma=\left(\frac{|\mathcal{E}_0|}{2U_p}\right)^{1/2}, \tag{24}$$

with U_p the ''ponderomotive potential'' $U_p=E^2/(4\omega^2)$, i.e., the mean quiver energy of an electron in the laser field, has to be much less than unity when tunneling theories such as ADK are derived. The Keldysh parameter has the vivid physical interpretation of tunneling time measured in units of the laser period. Does the Keldysh parameter reveal some significance in the BSI regime too? First of all we note that the Keldysh parameter in our numerical examples is not much less than unity. In the $\hat{E}=0.3$, $\omega=0.2$ case it is 0.67, in the $\hat{E}=0.5$, $\omega=0.1$ case it is 0.2. Thus, in commonly used terms in this field, we are rather in the multiphoton than in the (to BSI extended) tunneling regime.

However, the static field rates in Fig. 1 are also well covered by our empirical rate. Additional test runs at intermediate frequencies yielded good agreement also. Thus the insensitivity of our BSI rate with respect to the laser frequency (from static fields up to $\omega=0.2$) shows that there seems to be no need to put much emphasis on the concept of the Keldysh parameter in BSI. However, we did not deal with frequencies $\geqslant|\mathcal{E}_0|$ in this paper. Moreover, a small laser frequency keeps the portion of already ionized probability density far away from the ionic nucleus most of the time since the excursion length is large. Therefore the ionization curves for smaller frequencies usually look ''cleaner'' since interference with parts of the wave function representing the already ionized electron is suppressed.

V. CONCLUSION

We conclude that even for the simplest atom we can think of, i.e., atomic hydrogen, none of the theories discussed in this paper predict correctly the ionization rate in short intense laser pulses reaching the BSI regime. Thus extrapolation of tunneling theories to BSI is not permitted. From the numerical results we deduce that a successful theory should take the influence of the strong laser field on the *inner atomic* dynamics into account. For quantum treatments of strong field ionization this means that one must not make the assumption that the initial state (to be plugged into the transition matrix element) evolves in time as if it was unperturbed (as is usually done in KFR-type theories). In classical theories (such as the one by Posthumus *et al.*) this corresponds to taking the effect of the laser field on the bound Kepler orbits into acount. However, since in either case, quantum or classical, this appears extremely hard to achieve, empirical rates from numerical simulations of strong field ionization are highly desirable and important as an ingredient for other simulation codes, e.g., in the field of laser-solid interaction [27–29].

In this paper an empirical formula for the BSI rate has been proposed. Our formula is not sensitive to pulse shapes and laser frequencies in a wide parameter range, especially when combined with a reliable tunneling formula for the weaker parts of the laser pulse.

ACKNOWLEDGMENTS

This work was supported in part by the European Commission through the TMR Network SILASI (Super Intense Laser Pulse-Solid Interaction), No. ERBFMRX-CT96-0043 and by the Deutsche Forschungsgemeinschaft (DFG) under Contract No. MU 682/3-1.

APPENDIX: NUMERICAL METHOD

Starting point is the TDSE (2). We follow the line of Kono *et al.* [20] and perform the substitution (4)

$$\Phi(\xi,z,t)=\sqrt{\lambda}\xi^{\lambda-1/2}\psi(\xi^\lambda,z,t),\quad \xi^\lambda=\rho, \tag{A1}$$

The normalization condition for $\Phi(\xi,z,t)$ simply is

$$\int_0^\infty d\xi\int_{-\infty}^{\infty}dz\,|\Phi(\xi,z,t)|^2=1, \tag{A2}$$

i.e., we have a ''Cartesian''-like volume element $d\xi\,dz$ for the normalization of Φ.

With

$$H(t)=K_\xi+K_z+V(t), \tag{A3}$$

$$K_\xi=-\frac{1}{2\lambda^2\xi^{2\lambda}}\left\{\xi^2\frac{\partial^2}{\partial\xi^2}-2(\lambda-1)\xi\frac{\partial}{\partial\xi}+\left(\lambda-\frac{1}{2}\right)^2\right\}, \tag{A4}$$

$$K_z=-\frac{1}{2}\frac{\partial^2}{\partial z^2}, \tag{A5}$$

$$V(t)=-\frac{Z}{\sqrt{\xi^{2\lambda}+z^2}}+\frac{m^2}{2\xi^{2\lambda}}+z\hat{E}(t)\sin(\omega t+\varphi), \tag{A6}$$

the TDSE for $\Phi(\xi,z,t)$ assumes the form

$$i\frac{\partial}{\partial t}\Phi(\xi,z,t)=H(t)\Phi(\xi,z,t). \tag{A7}$$

The goal is to solve this TDSE.

If $\lambda>1/2$ the transformation (A1) implies that $\Phi(0,z,t)=0$ for all times. We discretize the (ξ,z) space by

$$\xi_j=j\Delta\xi,\quad j=1,2,\ldots,J,$$

$$z_k=(k-K/2)\Delta z,\quad k=1,2,\ldots,K \tag{A8}$$

with constant $\Delta\xi$ and Δz. While $\lambda=1$ yields the usual cylindrical coordinate system $\lambda=3/2$ turned out to offer the numerically more appropriate choice [20]. This is owing to the proper treatment of the wave function near the origin when the finite difference formulas for the first and second derivatives in the Hamiltonian (A3) are applied to the wave function Φ. Note that uniform spacing in ξ corresponds to nonuniform spacing in ρ. For $\lambda>1$ the ρ grid width near the origin is smallest while it gets coarser far away from the origin.

We use three-point-difference formulas for all derivatives in K_z and K_ξ and impose as additional boundary conditions

$$\Phi(\xi_J,z,t)=\Phi(\xi,z_1,t)=\Phi(\xi,z_K,t)=0. \tag{A9}$$

In longer runs we apply a filter each time step which removes probability density moving towards the boundaries. This is a somewhat ''shabby'' method (similar to ''imaginary potentials'') but proper ''absorbing boundary conditions'' as discussed in [25] are not easily implemented in more than one dimension. In any case, we always checked our numerical results upon sensitivity with respect to grid size and spacing.

The time propagation is performed by applying the evolution operator

$$U(t+\Delta t)=\frac{1}{[1+i\Delta tA(t_{n+1/2})/2]}\left(\frac{1-i\Delta tB(t_{n+1/2})/2}{1+i\Delta tB(t_{n+1/2})/2}\right)\times[1-i\Delta tA(t_{n+1/2})/2], \tag{A10}$$

with

$$A(t)=K_z+\frac{1}{2}V(t),\quad B(t)=K_\xi+\frac{1}{2}V(t)$$

to the discretized representation of $\Phi(\xi,z,t)$. This is the so-called Peaceman-Rachford (PR) method [26], the alternating direction version of the Crank-Nicholson method for the TDSE in more than one dimension. The evolution operator (A10) is second order accurate in time and space (as long as the usual three-point-difference formulas for the derivatives are used). Provided a noniterative method for solving the implicit matrix equations

$$[1+i\Delta tB(t_{n+1/2})/2]\Phi^{n+1/2}=[1-i\Delta tA(t_{n+1/2})/2]\Phi^n, \tag{A11}$$

$$[1+i\Delta tA(t_{n+1/2})/2]\Phi^{n+1}=[1-i\Delta tB(t_{n+1/2})/2]\Phi^{n+1/2} \tag{A12}$$

is chosen, the method is unconditionally stable.

The stable ground state on our numerical grid was determined by propagating a ''seed function'' in imaginary time, i.e., we substituted $\Delta t\rightarrow -i\Delta t$ in Eq. (A10). Here, renormalization of the wave function according to Eq. (A2) after several time steps is necessary since imaginary time propagation is not unitary. Our experience was that during imaginary time propagation Δt had to be sufficiently small for Φ converging to the ground state. A typical choice of our numerical parameters was (both for real and imaginary time propagation)

$$\Delta\xi=\Delta z=0.1,\quad \Delta t=0.05,\quad J=60,\quad K=1000.$$

[1] *Laser Interactions with Atoms, Solids, and Plasmas*, Vol. 327 of *NATO Advanced Study Institute Series B: Physics*, edited by Richard M. More (Plenum, New York, 1994).

[2] S. Augst, D. D. Meyerhofer, D. Strickland, and S. L. Chin, J. Opt. Soc. Am. B **8**, 858 (1990).

[3] Jianping Zhou, Greg Taft, Chung-Po Huang, Margaret M. Murnane, Henry C. Kapteyn, and Ivan P. Christov, Opt. Lett. **19**, 1149 (1994).

[4] A. Stingl, M. Lenzner, Ch. Spielmann, F. Krausz, and R. Szipöcs, Opt. Lett. **20**, 602 (1995).

[5] Jianping Zhou, Chung-Po Huang, Margaret M. Murnane, and Henry C. Kapteyn, Opt. Lett. **20**, 64 (1995).

[6] C. P. J. Barty, T. Guo, C. Le Blanc, F. Raksi, C. Rose-Petruck, J. Squier, K. R. Wilson, V. V. Yakovlev, and K. Yamakawa, Opt. Lett. **21**, 668 (1996).

[7] D. Bauer, Ph.D. thesis, Technische Hochschule Darmstadt, 1997.

[8] Kenneth J. Schafer and Kenneth C. Kulander, Phys. Rev. Lett. **78**, 638 (1997).

[9] E. E. Fill and G. Pretzler, in *Multiphoton Processes 1996*, edited by P. Lambropoulos and H. Walther, IOP Conf. Proc. No. 154 (Institute of Physics and Physical Society, Bristol, 1997), p. 10.

[10] M. V. Ammosov, N. B. Delone, and V. P. Krainov, Zh. Éksp. Teor. Fiz. **91**, 2008 (1986) [Sov. Phys. JETP **64**, 1191 (1987)].

[11] L. V. Keldysh, Zh. Éksp. Teor. Fiz. **47**, 1945 (1964) [Sov. Phys. JETP **20**, 1307 (1965)].

[12] Howard R. Reiss, Phys. Rev. A **22**, 1786 (1980); F. H. M. Faisal, J. Phys. B **6**, L89 (1973).

[13] L. D. Landau and E. M. Lifshitz, *Quantum Mechanics*, 3rd revised ed. (Pergamon, Oxford, 1977), p. 294.

[14] V. P. Krainov, in *Multiphoton Processes 1996*, edited by P. Lambropoulos and H. Walther, IOP Conf. Proc. No. 154 (Institute of Physics and Physical Society, Bristol, 1997), p. 98.

[15] J. H. Posthumus, M. R. Thompson, L. F. Frasinski, and K. Codling, in *Multiphoton Processes 1996* (Ref. [9]), p. 298.

[16] P. Mulser, A. Al-Khateeb, D. Bauer, A. Saemann, and R. Schneider, in *Laser Interaction and Related Plasma Phenomena*, Proceedings of the 12th International Conference, Osaka, 1995, edited by S. Nakai and G. H. Miley, AIP Conf. Proc. No. 369 (AIP Press, Woodbury, NY, 1996), pp. 565–575.

[17] Farhad H. M. Faisal, *Theory of Multiphoton Processes* (Plenum Press, New York, 1987), p. 8.

[18] One atomic mass unit $=m_e=9.1094\times10^{-31}$ kg; one atomic charge unit $=e=1.6022\times10^{-19}$ C; one atomic action unit $=\hbar=1.0546\times10^{-34}$ J s; one atomic length unit $=0.5292\times10^{-10}$ m (Bohr radius); one atomic energy unit $=27.21$ eV; one atomic field strength unit $=5.1422\times10^{11}$ V/m; one atomic time unit $=0.024$ fs; one atomic frequency (or rate) unit $=4.1341\times10^{16}$ s^{-1}; one atomic intensity unit $=3.5095\times10^{16}$ W/cm^2. The following formula useful is for practical purposes; it converts a given field amplitude (given in atomic units) into intensity (in W/cm^2): $I(\mathrm{W/cm^2})=3.51\times10^{16}\times\hat{E}^2(\mathrm{a.u.})$.

[19] Kenneth C. Kulander, Phys. Rev. A **35**, 445 (1987).

[20] Hirohiko Kono, Akihisa Kita, Yukiyoshi Ohtsuki, and Yuichi Fujimura, J. Comput. Phys. **130**, 148 (1997).

[21] U. Schwengelbeck and F. H. M. Faisal, Phys. Rev. A **50**, 632 (1994).

[22] Note that equating the ground-state energy level to the maximum of the barrier formed by the Coulomb potential and the external field leads to an underestimated critical field strength because the Stark shift does not vanish for a classical orbit in general.
[23] Robin Shakeshaft, R. M. Potvliege, Martin Dörr, and W. E. Cooke, Phys. Rev. A **42**, 1656 (1990).
[24] D. Bauer, Phys. Rev. A **55**, 2180 (1997).
[25] K. Boucke, H. Schmitz, and H.-J. Kull, Phys. Rev. A **56**, 763 (1997).
[26] S. E. Koonin, K. T. R. Davies, V. Maruhn-Rezwani, H. Feldmeier, S. J. Krieger, and J. W. Negele, Phys. Rev. C **15**, 1359 (1977).
[27] D. Bauer, R.R.E. Salomaa, and P. Mulser, Phys. Rev. E **58**, 2436 (1998).
[28] P. Mulser, F. Cornolti, and D. Bauer, Phys. Plasmas (to be published December 1998).
[29] F. Cornolti, A. Macchi, and E.C. Jarque, in *Superstrong Fields in Plasmas*, Proceedings of the First International Conference, Varenna, Italy, 1997, edited by M. Lontano, G. Mourou, F. Pegoraro, and E. Sindoni, AIP Conf. Proc. No. 426 (AIP, Woodbury, NY, 1998), p. 55.